[redacted]

Copy
SL54E14

NACA

[redacted]

SL54E14

RESEARCH MEMORANDUM

for the

U. S. Air Force

FLIGHT RESULTS FROM A 1/10-SCALE ROCKET MODEL OF THE LOCKHEED XF-104 AIRPLANE AT TRANSONIC MACH NUMBERS

By Alan B. Kehlet

Langley Aeronautical Laboratory
Langley Field, Va.

NATIONAL ADVISORY COMMITTEE FOR AERONAUTICS

WASHINGTON

MAY 14 1954

NATIONAL ADVISORY COMMITTEE FOR AERONAUTICS

RESEARCH MEMORANDUM

for the

U. S. Air Force

FLIGHT RESULTS FROM A 1/10-SCALE ROCKET MODEL OF THE LOCKHEED XF-104 AIRPLANE AT TRANSONIC MACH NUMBERS

By Alan B. Kehlet

SUMMARY

A 1/10-scale rocket model of the Lockheed XF-104 with faired inlets has been flown over a Mach number range from 0.80 to 1.45 to determine low-lift drag and a limited amount of stability data. The center-of-gravity locations were 4.0 and 1.5 percent of the mean aerodynamic chord before and after sustainer firing, respectively. Oscillations induced by pulse rockets were used to determine stability data.

The external transonic drag coefficient increased from a value of 0.0160 at Mach number 0.80 to a maximum of 0.0432 near Mach number 1.13, with a drag rise Mach number of about 0.93. At Mach numbers where it could be determined, the model exhibited stable dynamic and static stability characteristics at low lift.

INTRODUCTION

At the request of the U. S. Air Force and in coordination with wind-tunnel programs, a 1/10-scale rocket model of the Lockheed XF-104 with faired inlets was flight tested to obtain low-lift drag data over a Mach number range from 0.80 to 1.45 and a Reynolds number range of 3.2 to 9.6×10^6. A limited amount of stability data were obtained during the first portion of the flight by the use of pulse rockets to disturb the model in pitch.

The model was flown at the Langley Pilotless Aircraft Research Station at Wallops Island, Va.

SYMBOLS

C_N	normal-force coefficient, $\frac{a_n}{g}\frac{W/S}{q}$
C_C	chord-force coefficient, $-\frac{a_l}{g}\frac{W/S}{q}$
C_m	pitching-moment coefficient about center of gravity
$C_{D_{ext}}$	external-drag coefficient, $C_C - C_{D_b}$
C_{D_b}	base-drag coefficient, $-C_{p_b}\frac{S_b}{S}$
C_{p_b}	base-pressure coefficient, $\frac{p_b - p}{q}$
C_{D_f}	friction drag coefficient, $C_f\left(\frac{S_w}{S}\right)$
C_f	flat plate viscous drag coefficient
a_n	normal acceleration determined from accelerometer, ft/sec^2
a_l	longitudinal acceleration determined from accelerometer, ft/sec^2
g	acceleration of gravity, ft/sec^2
q	dynamic pressure, $0.7pM^2$
p	free-stream static pressure, lb/sq ft
M	Mach number
dC_D/dM	rate of change of drag coefficient with Mach number
W	weight, lb

p_b base pressure, lb/sq ft

S wing area (including area enclosed by fuselage), sq ft

S_w wetted area, sq ft

S_b base area, sq ft

R Reynolds number, based on wing mean aerodynamic chord

$\bar{c}$ wing mean aerodynamic chord (M.A.C.), ft

A cross-sectional area, sq in.

r radius of equivalent cross-sectional area, in., $\sqrt{A/\pi}$

x longitudinal distance from station 0, in.

l length of model, in.

$T_{1/2}$ time to damp to one-half amplitude, sec

θ angle of pitch, radians

C_{m_α} $\frac{dC_m}{d\alpha}$, per deg

α angle of attack, deg

C_{m_q} $\frac{dC_m}{d\left(\frac{q\bar{c}}{2V}\right)}$, per radian

$C_{m_{\dot{\alpha}}}$ $\frac{dC_m}{d\left(\frac{\dot{\alpha}\bar{c}}{2V}\right)}$, per radian

$\dot{\alpha}$ $\frac{1}{57.3}\frac{d\alpha}{dt}$

q $\frac{d\theta}{dt}$ when used in damping term

V velocity, ft/sec

MODEL AND INSTRUMENTATION

Model

A three-view drawing of the model is shown in figure 1. The nondimensional equivalent body and area distribution at $M = 1.0$ are shown in figure 2. Photographs of the model are shown in figure 3. The rocket model, as furnished by Lockheed Aircraft Corporation, was constructed throughout of cast aluminum-magnesium alloy with the exception of the duct fairing blocks which were of cast tin-bismuth alloy.

The external contours of the rocket model differed from the airplane only in the basic fuselage. For a fuselage, the rocket model had a body of revolution (the radii of which were scaled from the cross-sectional areas of the airplane basic fuselage) with a canopy and faired ducts added. The wing had an aspect ratio of 2.50, an unswept 70 percent chord line, and a modified biconvex airfoil section (thickness ratio of 3.4 percent) perpendicular to the chord plane. A table of ordinates is given in table 1. The horizontal tail had an aspect ratio of 2.93, thickness ratios of 5 percent at the root and 3 percent at the tip, and a modified biconvex airfoil section (table 2). The incidence was fixed at 1.5°, trailing edge down.

With the 2.25-inch-diameter AR sustainer motor loaded, the model weighed 106.9 pounds, had a center-of-gravity location at 4 percent $\bar{c}$, and a moment of inertia of 3.450 slug-ft^2. After sustainer firing, the corresponding mass characteristics were 105.0 pounds and 3.425 slug-ft^2 with center-of-gravity location at 1.5 percent $\bar{c}$.

Three vertically thrusting pulse rockets with total impulse of approximately 8 pound-seconds each and burning time of approximately 0.08 second were installed in the model at a longitudinal location as shown in figure 1.

Instrumentation

The model was equipped with an NACA four-channel telemeter which transmitted continuous records of normal and logitudinal acceleration, total pressure, and base pressure. The four base-pressure orifices (fig. 3(b)) were joined to give a single pressure measurement.

Flight path and velocity information were obtained from space and Doppler radar units, respectively. Atmospheric conditions were obtained from a radiosonde released shortly before the flight. Motion-picture cameras were used to photograph the launching and first portion of the flight.

TESTS AND DATA REDUCTION

Flight Tests

The rocket model was launched at an angle of approximately 60° from the horizontal by means of a mobile launcher as shown in figure 3(c). A 6-inch-diameter solid-fuel ABL Deacon rocket motor boosted the model to maximum velocity. At booster burn-out, the model-booster combination separated and the model decelerated. A short time after separation, the 2.25-inch-diameter sustainer rocket motor fired (primarily to assist in tracking) so that the model was accelerated to near maximum velocity.

Data Reduction

The technique of data reduction for analyzing the response of models to pulse rocket disturbances is described in reference 1; that is, static longitudinal stability is determined from the periods of the short-period oscillations and dynamic longitudinal stability is determined from the rate of decay of the oscillations. The oscillations occurring during pulse rocket burning are not included in the analysis because the time history of the thrust-forcing function cannot be evaluated accurately.

The trim lift and drag were determined between pulses directly from the telemetered data and through oscillations by the appropriate fairing.

All data, with the exception of some trim, were taken during the decelerating portion of the flight.

Accuracy

The absolute accuracy of the measured quantities is impossible to establish because the instrument calibration cannot be checked during or after the flight. An indication of the maximum systematic instrument errors possible is given by the following table, based on an accuracy of ±1 percent of the full-scale instrument range:

M	C_N	C_C
0.9	±0.0141	±0.0047
1.3	±.0050	±.0016

Based on comparisons of telemetered and Doppler drag-coefficient data of reference 2, the probable errors are believed to be much less than the systematic errors indicate.

Mach number is believed to be accurate to ±0.01 at $M = 1.00$.

RESULTS AND DISCUSSION

Dynamic pressure and Reynolds number obtained during the flight are shown as a function of Mach number in figure 4. A typical portion of the time history of the quantities measured from the model is shown in figure 5.

Drag

The variation of the rocket-model drag coefficients at trimmed lift conditions as a function of Mach number is shown in figure 6. Included in the figure for comparative purposes, are the estimated friction-drag-coefficient data determined by means of reference 3.

The chord-force coefficient is used herein as the total drag coefficient. This usage results in a small error since the data were not corrected for lift coefficient and angle of attack; however, since the model was flown at low lift coefficients and probably low angles of attack, the two quantities should be almost equal.

The total-drag coefficient (C_C) was obtained directly from the longitudinal accelerometer, the base-drag coefficient from the single pressure reading of the four base orifices (fig. 3), and the external-drag coefficient from an algebraic subtraction of the total-drag and base-drag coefficients. Although the external-drag coefficient contains no correction for internal-flow drag, unpublished wind-tunnel data indicated little difference in external drag with ducts open or faired for this particular configuration.

At transonic Mach numbers, the external-drag coefficient increased from a value of 0.0160 at $M = 0.80$ to a maximum of 0.0432 near $M = 1.13$ with a drag-rise Mach number $\left(\frac{dC_D}{dM} = 0.1\right)$ of about $M = 0.93$.

The hook in the curve and the subsequent increase in abruptness of the drag rise near $M = 0.98$ are believed due to pressure changes on the rear fuselage and have been noted previously on similar fuselage shapes (ref. 2).

The external trimmed drag coefficient and the estimated friction-drag coefficient are in good agreement at $M = 0.80$, with values of 0.0160 and 0.0150, respectively.

Longitudinal Trim

The variation of the rocket-model trim normal-force coefficient with Mach number is shown in figure 7. At supersonic Mach numbers, the model trimmed near a normal-force coefficient of 0.03. No data were obtained between Mach numbers from 0.99 to 1.225 because of failure of the normal accelerometer channel, which "went into noise" at about $M = 1.225$. Later in the flight, the channel signal returned. The "probable trim" data shown at transonic Mach numbers were obtained after the model had passed its apogee and was accelerating due to gravity on the downward portion of the flight. The values of the probable trim data should not be considered absolute due to the generally decreased accuracy of the measured quantities so late in the flight; however, calculated transonic trim values from unpublished wind-tunnel data agree very closely with the rocket-model data in both magnitude and shape.

Longitudinal Static and Dynamic Stability

A summary plot of the longitudinal stability parameters at Mach numbers for which they could be determined is shown as figure 8. The lift-curve slopes from reference 4 which are presented, were used in the determination of the aerodynamic center and the pitch damping-moment factors, $C_{m_q} + C_{m_{\dot{\alpha}}}$. As a result of the failure of the normal accelerometer, the static stability data at $M = 1.165$ were determined from the periods of the oscillations of the base pressure. Damping of this oscillation was not believed to be the realistic model damping and was not used; however, the resulting error in the static stability parameter C_{m_α} because of the absence of the damping term is negligible at this Mach number.

The configuration is shown to be longitudinally stable over the Mach number and lift-coefficient range covered for the center-of-gravity locations used. The degree of longitudinal stability, as indicated by the aerodynamic-center location, is also shown on the figure. Whereas the static stability parameter C_{m_α} was essentially constant over the Mach number range covered, the aerodynamic center moved rearward with increasing Mach number.

Included in the figure are values of the time to damp to one-half amplitude and the pitch damping-moment factors corresponding to these time increments. The damping is stable over the Mach number and lift-coefficient range covered by the oscillations.

CONCLUSIONS

Drag and stability results from a 1/10-scale rocket model of the Lockheed XF-104 with faired inlets indicate the following conclusions:

1. The drag-rise Mach number was about 0.93 and the trimmed transonic external drag coefficient increased from 0.0160 at $M = 0.80$ to a maximum of 0.0432 near $M = 1.13$.

2. For a tail setting of 1.5° trailing edge down, the model trimmed near zero lift for the range of supersonic Mach numbers covered by the test and at slightly negative lift coefficients for the subsonic Mach numbers.

3. At supersonic speeds and at low lift coefficients, the model exhibited stable longitudinal stability characteristics.

Langley Aeronautical Laboratory,
National Advisory Committee for Aeronautics,
Langley Field, Va., May 3, 1954.

Alan B. Kehlet

Alan B. Kehlet
Aeronautical Research Scientist

Approved:

Paul R. Hill

for Joseph A. Shortal
Chief of Pilotless Aircraft Research Division

cg

REFERENCES

1. Parks, James H., and Kehlet, Alan B.: Longitudinal Stability, Trim, and Drag Characteristics of a Rocket-Propelled Model of an Airplane Configuration Having a 45° Sweptback Wing and an Unswept Horizontal Tail. NACA RM L52F05, 1952.

2. Morrow, John D., and Nelson, Robert L.: Large-Scale Flight Measurements of Zero-Lift Drag of 10 Wing-Body Configurations at Mach Numbers from 0.8 to 1.6. NACA RM L52D18a, 1953.

3. Van Driest, E. R.: Turbulent Boundary Layer in Compressible Fluids. Jour. Aero. Sci., vol. 18, no. 3, Mar. 1951, pp. 145-160, 216.

4. Mandel, M. W., Mayer, F. S., Waugh, M. G., and Tseu, P. S.: Stability and Control of the XF-104. LAL Rep. No. 8997, Lockheed Aircraft Corp., April 13, 1953.

TABLE 1.- WING CONTOUR ORDINATES 4.00 INCHES

FROM FUSELAGE CENTER LINE

Percent chord	Horizontal distance, in.	± Vertical distance, in.
-1.25	-1.54	0
0	0	0
.25	.031	.021
.50	.062	.030
1.25	.154	.047
2.50	.308	.065
5.00	.616	.091
10.00	1.233	.126
15.00	1.849	.150
20.00	2.466	.168
25.00	3.082	.181
30.00	3.699	.192
35.00	4.315	.200
40.00	4.932	.205
45.00	5.548	.208
50.00	6.165	.210
55.00	6.781	.207
60.00	7.398	.201
65.00	8.014	.191
70.00	8.631	.176
75.00	9.247	.157
80.00	9.864	.134
85.00	10.480	.107
90.00	11.097	.076
95.00	11.713	.041
100.00	12.330	.004

TABLE 2.- HORIZONTAL TAIL CONTOUR ORDINATES

0.50 INCH FROM FUSELAGE CENTER LINE

Percent chord	Horizontal distance, in.	± Vertical distance, in.
-1.25	-0.087	0
0	0	0
.25	.017	.017
.50	.035	.024
1.25	.087	.038
2.50	.174	.054
5.00	.347	.074
10.00	.695	.103
15.00	1.042	.122
20.00	1.390	.137
25.00	1.737	.149
30.00	2.084	.157
35.00	2.432	.163
40.00	2.779	.168
45.00	3.127	.171
50.00	3.474	.172
55.00	3.821	.170
60.00	4.169	.164
65.00	4.516	.155
70.00	4.864	.145
75.00	5.211	.128
80.00	5.558	.109
85.00	5.906	.087
90.00	6.253	.062
95.00	6.601	.034
100.00	6.948	.004

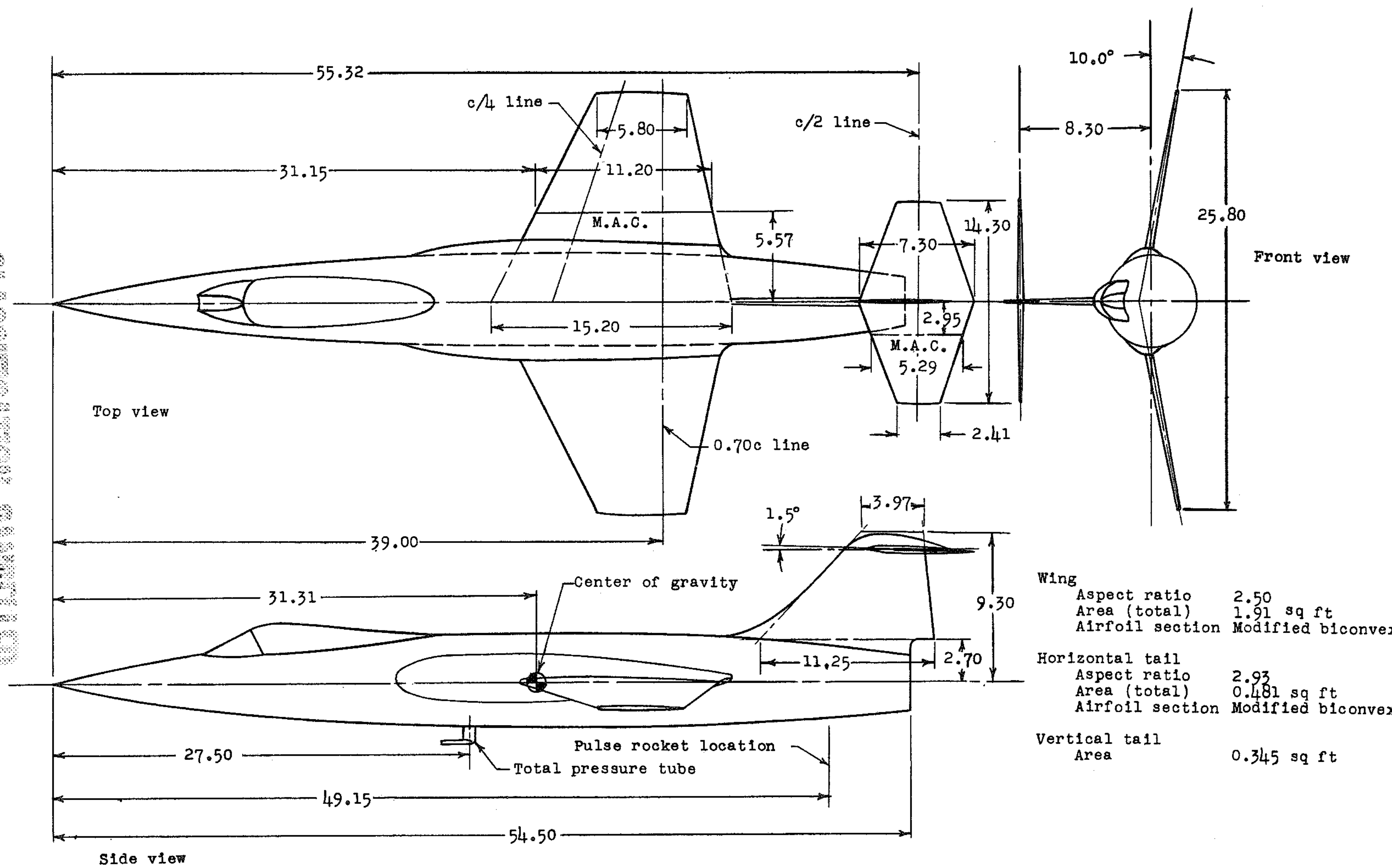

Figure 1.- General arrangement of 1/10-scale rocket model. All dimensions are in inches.

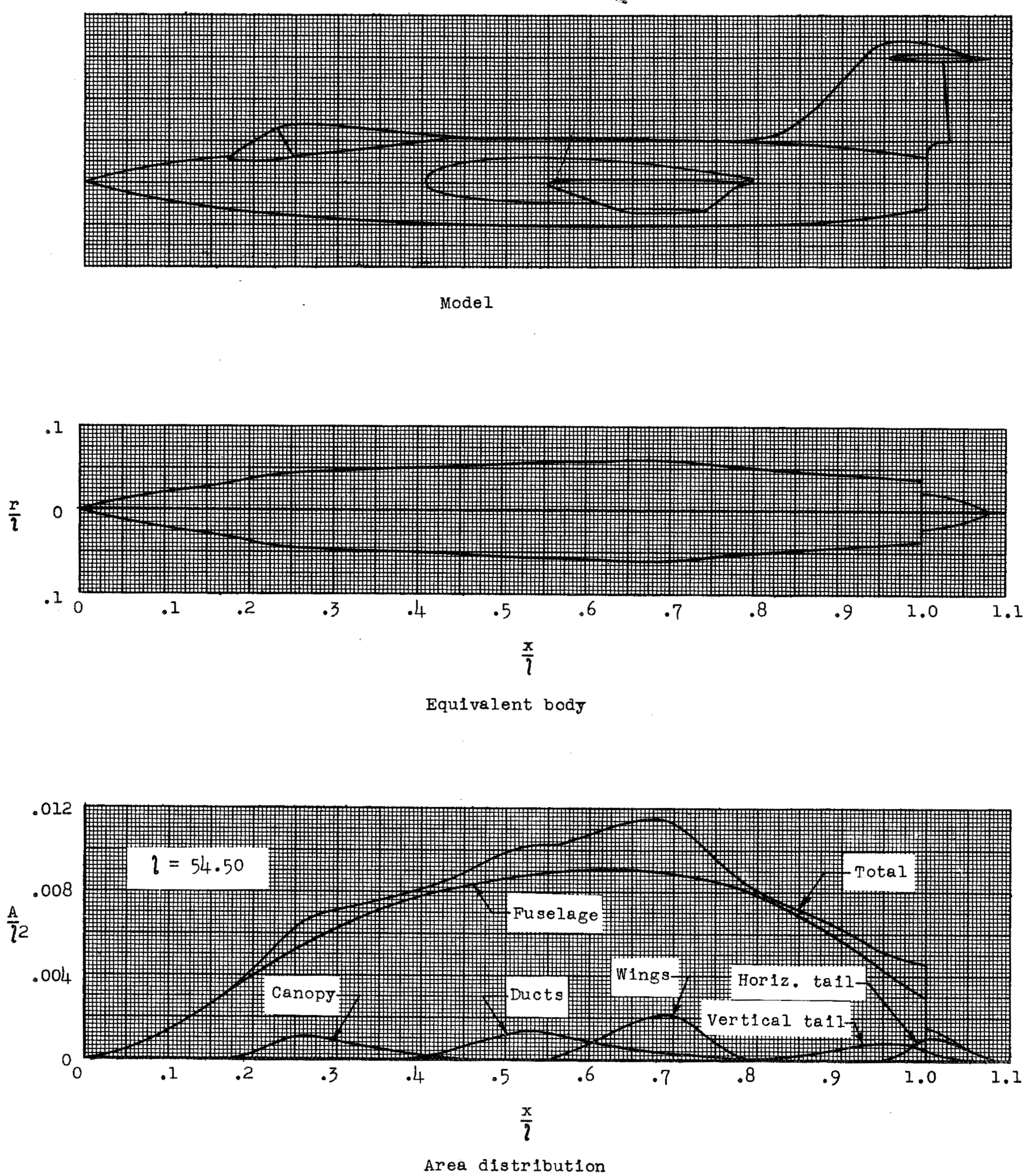

Figure 2.- Nondimensional equivalent body and area distribution of model at M = 1.0.

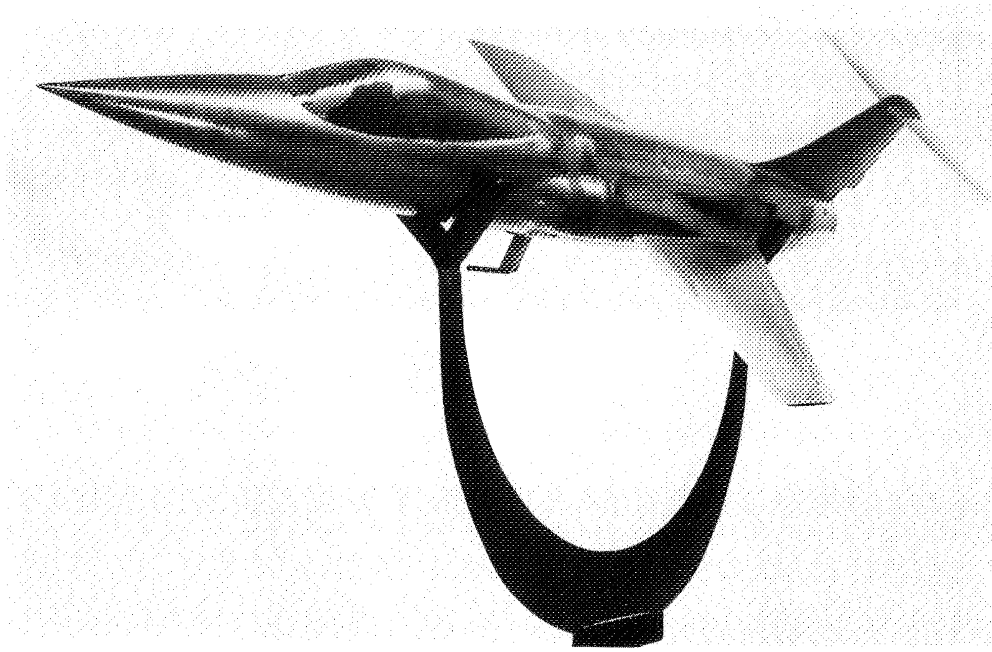

L-82678.1

(a) Three-quarter front view.

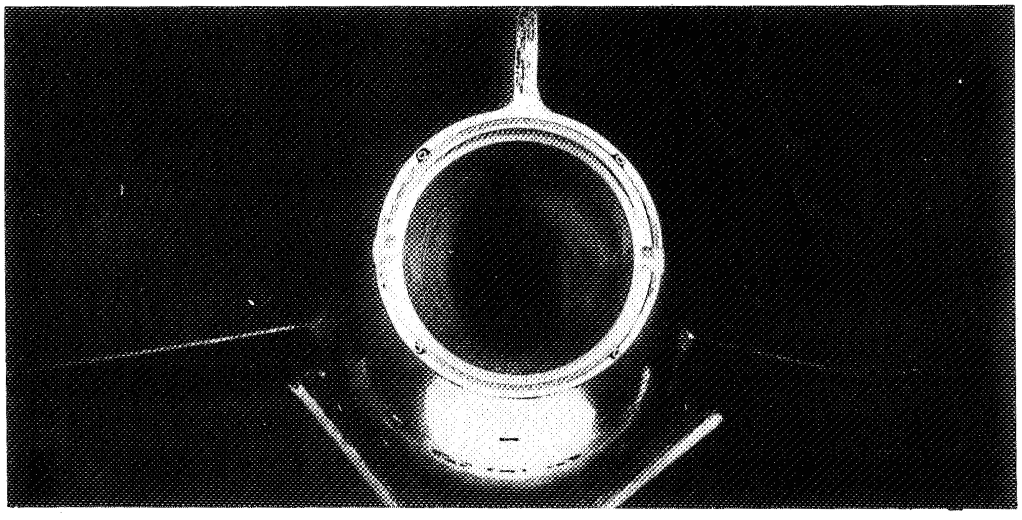

L-82680

(b) Rear view showing base pressure orifices.

Figure 3.- Photographs of model.

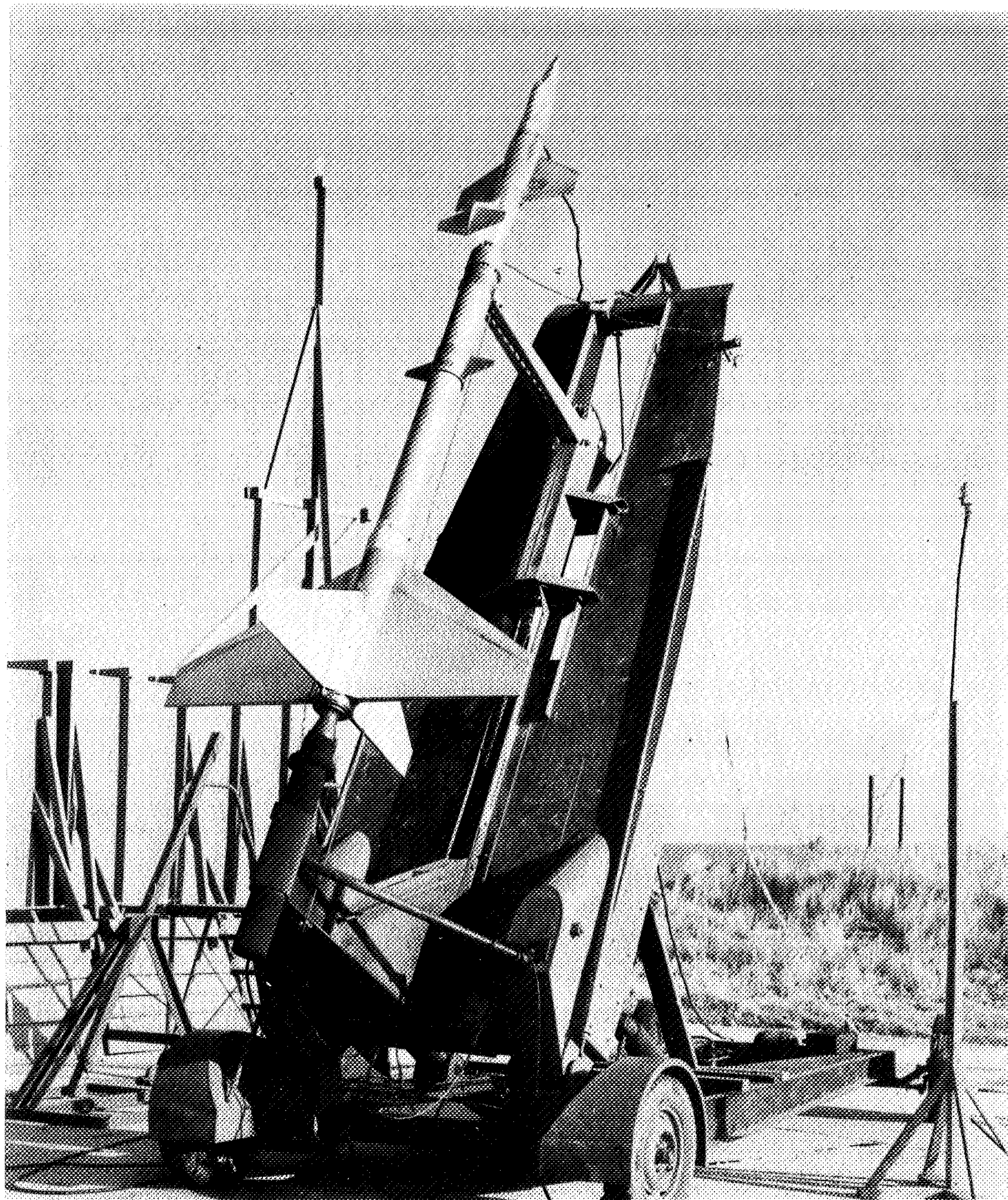

L-83115.1

(c) Model on launcher.

Figure 3.- Concluded.

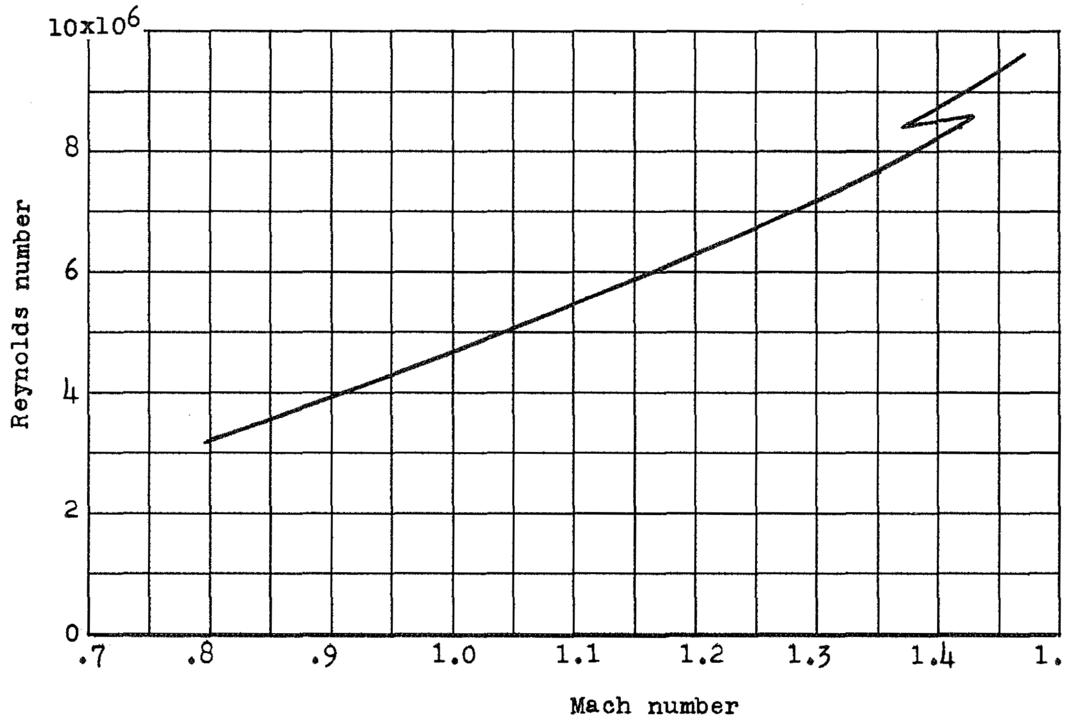

(a) Reynolds number.

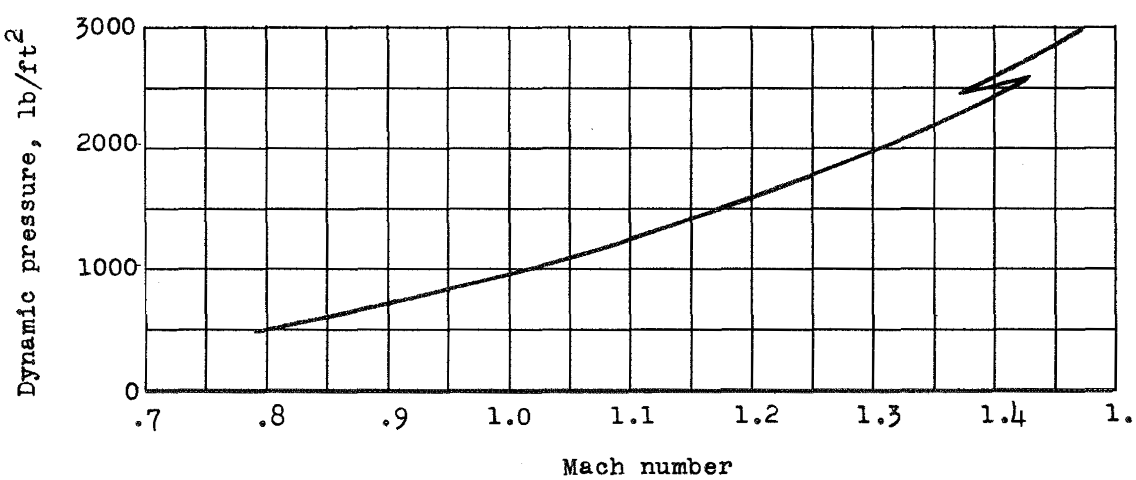

(b) Dynamic pressure.

Figure 4.- Variation of Reynolds number and dynamic pressure with Mach number.

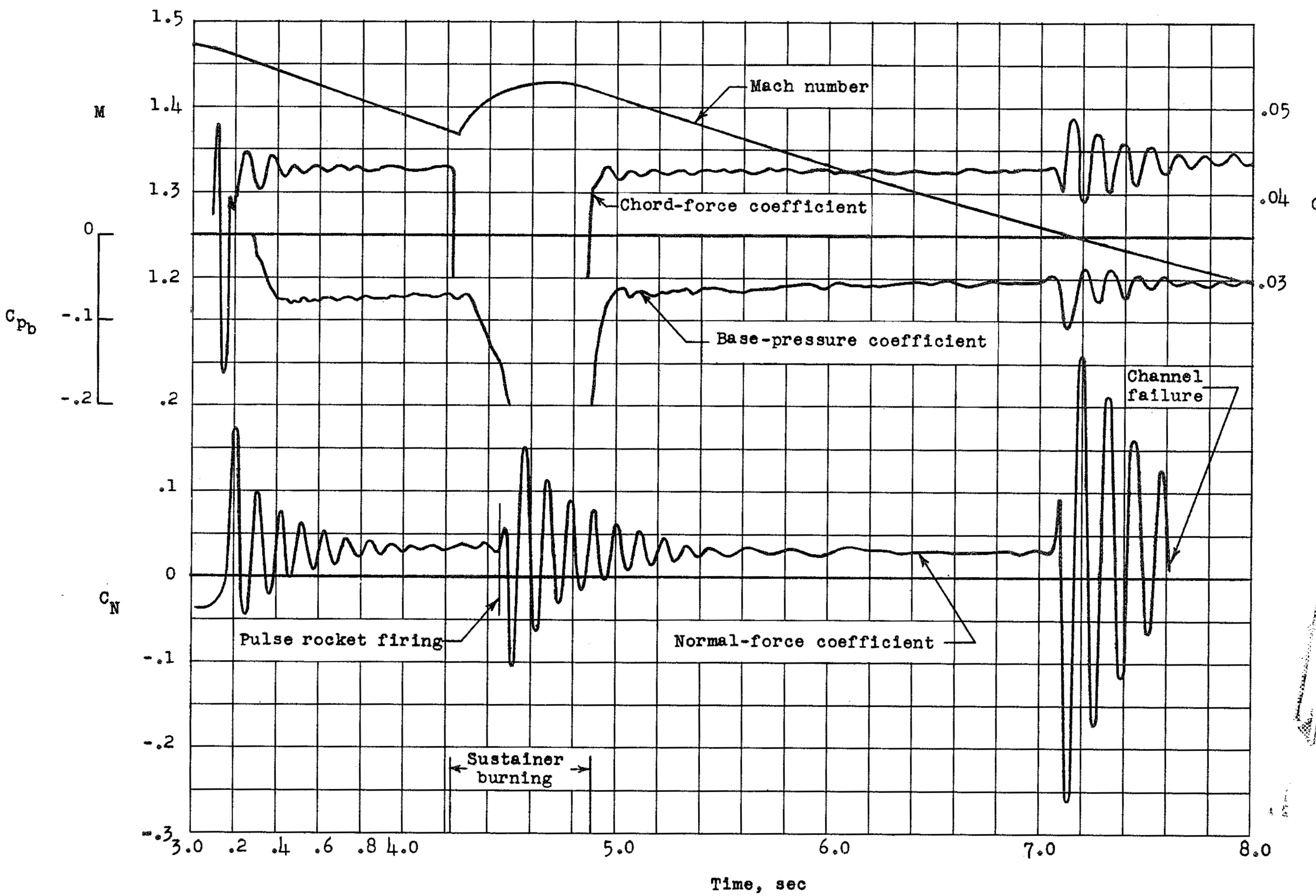

Figure 5.- Time history during first portion of flight of quantities obtained in present investigation.

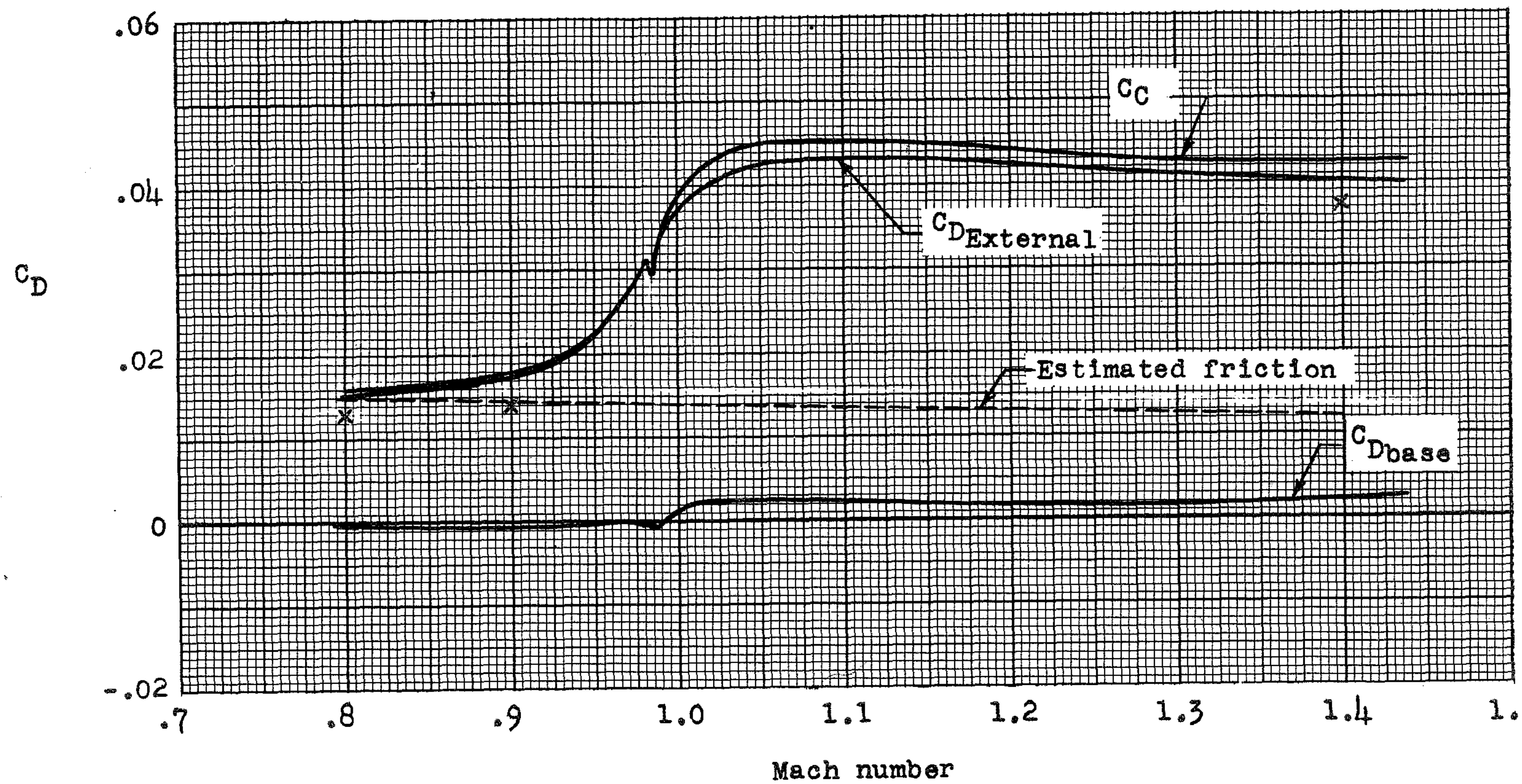

Figure 6.- Variation of drag coefficients with Mach number.

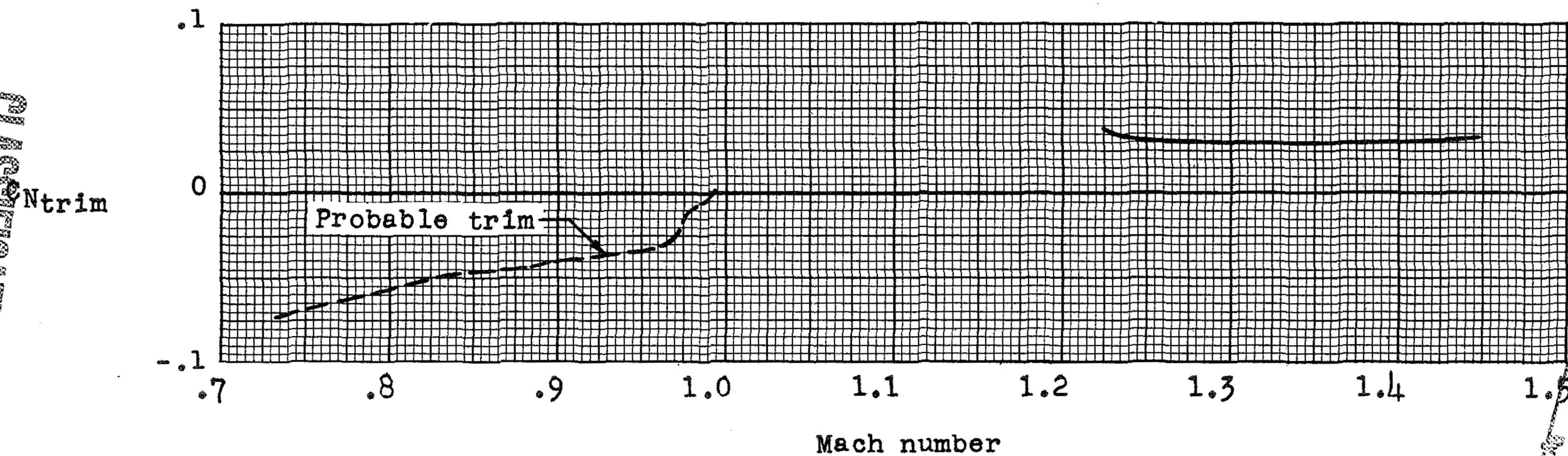

Figure 7.- Variation of trim normal-force coefficient with Mach number.

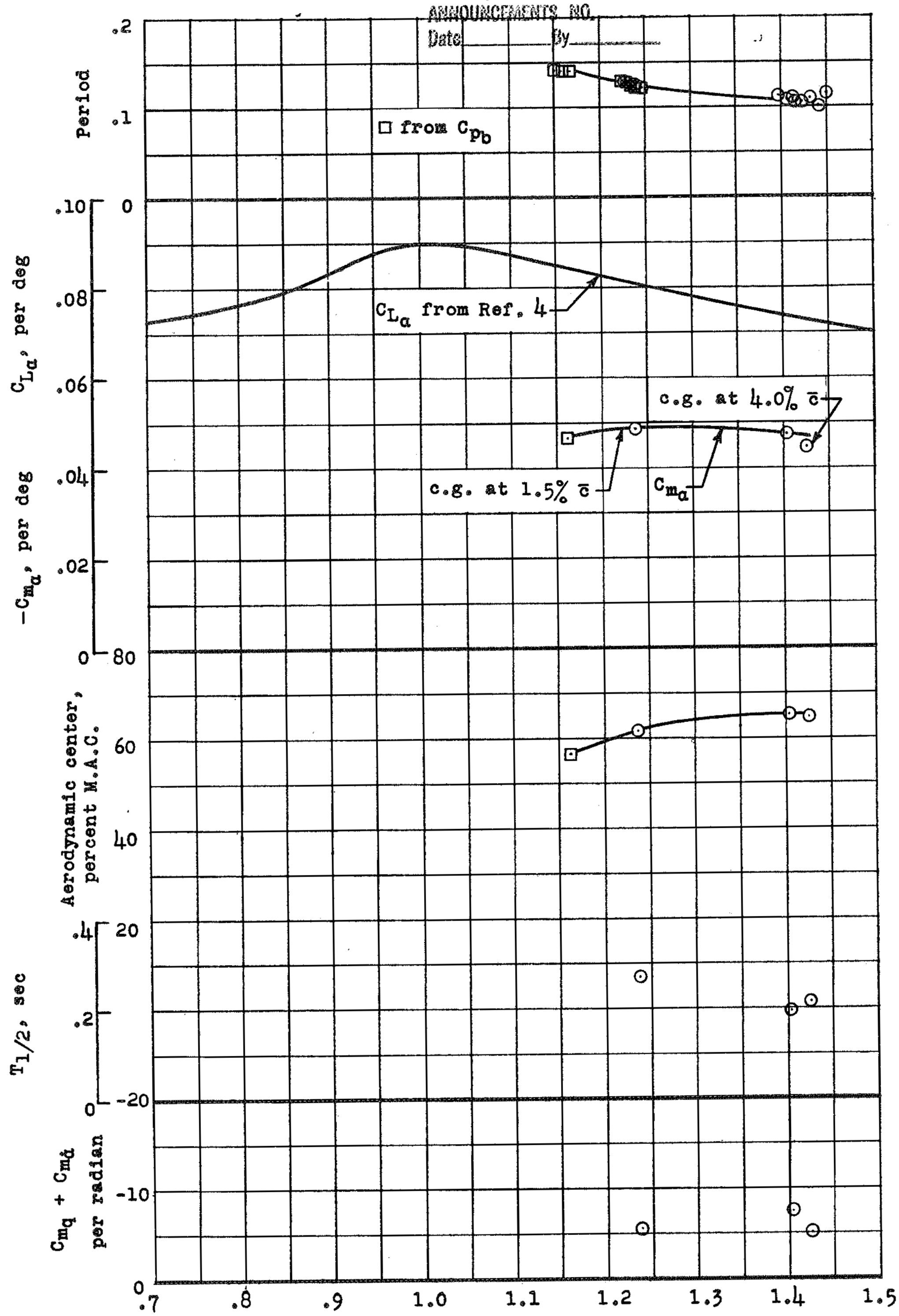

Figure 8.- Summary of static and dynamic longitudinal stability parameters as functions of Mach number.